ApJ, in press
Preprint typeset using LaTeX style emulateapj v. 8/13/10

CHANDRA AND *RXTE* OBSERVATIONS OF 1E 1547.0−5408: COMPARING THE 2008 AND 2009 OUTBURSTS

C.-Y. Ng[1], V. M. Kaspi, R. Dib, S. A. Olausen, P. Scholz
Department of Physics, McGill University, Montreal, QC H3A 2T8, Canada

T. Güver, F. Özel
Department of Astronomy, University of Arizona, Tucson, AZ, 85721

F. P. Gavriil
NASA Goddard Space Flight Center, Astrophysics Science Division, Code 662, Greenbelt, MD 20771 and
Center for Research and Exploration in Space Science and Technology, University of Maryland Baltimore County, Baltimore, MD 21250

and

P. M. Woods
Corvid Technologies, Huntsville, AL 35806
ApJ, in press

ABSTRACT

We present results from *Chandra X-ray Observatory* and *Rossi X-ray Timing Explorer* (*RXTE*) observations of the magnetar 1E 1547.0−5408 (SGR J1550−5418) following the source's outbursts in 2008 October and 2009 January. During the time span of the *Chandra* observations, which covers days 4 through 23 and days 2 through 16 after the 2008 and 2009 events, respectively, the source spectral shape remained stable in the *Chandra* band, while the pulsar's spin-down rate in the same span in 2008 increased by a factor of 2.2 as measured by *RXTE*. This suggests decoupling between the source's spin-down and radiative changes, hence between the spin-down-inferred magnetic field strength and that inferred spectrally. The lack of spectral variation during flux decay is surprising for models of magnetar outbursts. We also found a strong anti-correlation between the phase-averaged flux and the pulsed fraction in the 2008 and 2009 *Chandra* data, but not in the pre-2008 measurements. We discuss these results in the context of the magnetar model.

Subject headings: pulsars: individual (1E 1547.0−5408, PSR J1550−5418, SGR J1550−5418) — stars: neutron — X-rays: bursts

1. INTRODUCTION

Anomalous X-ray pulsars (AXPs) and soft gamma repeaters (SGRs), though previously thought to be different classes of objects, are now believed to all be strongly magnetized neutron stars, known as "magnetars". They are characterized by long spin periods of 2-12 s and large spin-down rates that imply ultra-strong surface dipole magnetic fields of 10^{14}-10^{15} G (see reviews by Kaspi 2007 and Mereghetti 2008). The most remarkable feature of magnetars is their violent outbursts, during which the X-ray luminosity could increase by a few orders of magnitude. In the context of the twisted magnetosphere model (Thompson et al. 2002), the energy release is due to magnetic field re-arrangement, which is possibly triggered by crustal deformation. While the post-outburst behavior of a magnetar can provide important information on the physical conditions of the magnetosphere and the stellar surface, only a handful of follow-up studies have previously been carried out with focusing X-ray instruments (e.g. Woods et al. 2004; Gavriil et al. 2006; Israel et al. 2007), because the transient nature of these events requires prompt observations. In this work, we study recent outbursts from the AXP 1E 1547.0−5408[2] in 2008 and 2009 using observations made with the *Chandra X-ray Observatory* and the *Rossi X-ray Timing Explorer* (*RXTE*).

The X-ray source 1E 1547.0−5408 was discovered by Lamb & Markert (1981) with the *Einstein Observatory*. Based on the X-ray spectrum and infrared flux, Gelfand & Gaensler (2007) first suggested the source as a magnetar candidate. The detection of radio pulsations by Camilo et al. (2007) directly confirmed the pulsar nature of this object; its spin period of 2.1 s is shorter than any other known magnetars.[3] The pulsar's spin-down rate as reported by Camilo et al. (2007) implies a surface magnetic dipole field of 2.2×10^{14} G. Halpern et al. (2008) reported a high state of this magnetar in 2007 based on *XMM-Newton* observations, and they concluded that an X-ray outburst had occurred between 2006 and 2007. On 2008 October 3 (MJD 54742), 1E 1547.0−5408 showed bursting activity with outbursts detected by *Swift* (Israel et al. 2010) and by the Gamma-ray Burst Monitor (GBM) onboard the *Fermi Gamma-ray Space Telescope* (Kaneko et al. 2010). On 2009 January 22 (MJD 54853), the AXP entered a second active

ncy@hep.physics.mcgill.ca
[1] Tomlinson Postdoctoral Fellow

[2] Also known as SGR J1550−5418 or PSR J1550−5418.
[3] See the online magnetar catalog at http://www.physics.mcgill.ca/~pulsar/magnetar/main.html.

TABLE 1
Chandra Observation Parameters and Results

Obs.	Date	MJD	ObsID	Days Since Outburst	Exposure (ks)	Count Rate[a] (s^{-1})	Pulsed Fraction[a]
			2008 October				
1	2008 Oct 7	54746.6	8811	4.2	12.1	1.35(1)	0.21(1)
2	2008 Oct 10	54749.5	8812	7.2	15.1	1.17(1)	0.22(1)
3	2008 Oct 18	54757.6	8813	15.2	10.1	1.15(1)	0.33(1)
4	2008 Oct 21	54760.8	10792	18.4	10.1	1.07(1)	0.35(1)
5	2008 Oct 26	54765.1	8814	22.8	23.0	0.99(1)	0.31(1)
			2009 January				
6	2009 Jan 23	54855.0	10185	2.0	10.1	0.95(1)[b]	0.09(1)
7	2009 Jan 25	54856.7	10186	3.7	12.1	3.1(2)	0.09(1)
8	2009 Jan 29	54860.8	10187	7.8	13.1	2.5(1)	0.13(1)
9	2009 Feb 06	54868.6	10188	15.6	14.3	2.2(1)	0.12(1)

[a] In the $1-7$ keV energy range.
[b] Obs. 6 was made with the HETG, which results in a reduced count rate. Correcting for the effective area gives a count rate of ~ 3.6.

phase. More than 200 bursts were detected within a few hours by *Swift*, *International Gamma-Ray Astrophysics Laboratory* (*INTEGRAL*), *Fermi* GBM, and *Suzaku* WAM (Gronwall et al. 2009; Mereghetti et al. 2009; Savchenko et al. 2010; Kaneko et al. 2010; Terada et al. 2009). Follow-up imaging observations with *Swift* and *XMM-Newton* revealed dust scattering-X-ray rings centered on the source, from which Tiengo et al. (2010) deduced a source distance of 3.9 kpc. Based on *Suzaku* observations taken 7 days after the 2009 outburst, Enoto et al. (2010) reported a hard power-law tail in the spectrum, of photon index Γ between 1.33 and 1.55, and extending up to at least 110 keV. Hard X-ray pulsations were also detected by *INTEGRAL* in the 20-150 keV band (Kuiper et al. 2009; den Hartog et al. 2009). The pulsed emission has $\Gamma = 1.55$ and the spectral shape remained stable over the observation period covering from day 2 to day 9 after the outburst.

In this paper, we report on results from *Chandra* and *RXTE* observations taken after the 2008 and 2009 events. The observations and results are reported in Section 2, and we discuss their physical implications in Section 3. We summarize our findings in Section 4.

2. OBSERVATIONS AND RESULTS

2.1. *RXTE Observations and Results*

Since the 2008 October outburst, 1E 1547.0−5408 has been monitored regularly with *RXTE*. Data are collected with the Proportional Counter Array (PCA) instrument that consists of five collimated xenon/methane multi-anode Proportional Counter Units (PCUs). Only `GoodXenonwithPropane` mode data were used in our analysis, which give 1 μs time resolution and 256 energy channels in the 2-60 keV energy range. We considered events from only the top Xenon layer of each PCU to maximize the signal-to-noise ratio (S/N). Typical exposure times were in the range 2–7 ks. In all, we report here on a total of 55 observations taken between MJDs 54743 and 54911. A more complete report on the *RXTE* data will be presented elsewhere (R. Dib et al., in preparation).

2.1.1. *RXTE Timing*

To determine the pulsar spin parameters, we cleaned the *RXTE* data and selected events between 2 and 6.5 keV. As the source exhibited many short X-ray bursts, we removed all burst intervals for this analysis. The photon arrival times were first corrected to the solar system barycenter, then binned with 31.25 ms time resolution. The time series were folded at the nominal spin period and pulse arrival times were extracted by cross-correlating with a template. These arrival times were then fitted to a simple phase-coherent timing model using the TEMPO software package.[4] Details on the phase folding and periodicity search techniques are described in Dib et al. (2009). Our best-fit timing solution gives a spin frequency $\nu = 0.48277818(5)$ Hz, frequency derivative $\dot{\nu} = -6.6(1)\times10^{-12}\,s^{-2}$, and second frequency derivative $\ddot{\nu} = -6.2(1)\times10^{-18}\,s^{-3}$ covering the 2008 *Chandra* epochs (reference epoch of MJD 54743.0), and $\nu = 0.4825962(4)$ Hz, $\dot{\nu} = -5.17(5)\times10^{-12}\,s^{-2}$ with negligible $\ddot{\nu}$ for the 2009 *Chandra* epochs (reference epoch of MJD 54854.0). These values are consistent with those reported by Israel et al. (2010) and Kaneko et al. (2010) based on the 2008 *Swift* and 2009 *Fermi* observations, respectively.

2.1.2. *RXTE Pulsed Fluxes*

Once the timing solution was obtained, we regenerated the pulse profiles in the 2-10 keV band, and calculated the rms pulsed flux according to the formula in Dib et al. (2008), using seven harmonics. The results are plotted in Figure 1 and reveal a complicated flux evolution. In this paper, we focus mainly on time periods near the *Chandra* epochs, and a full analysis of the *RXTE* data will be presented by R. Dib et al. (in preparation). Approximately 11 days after the initial 2008 October 3 (MJD 54742) trigger, during which the pulsed flux decayed roughly monotonically, the pulsed emission abruptly increased again by 80% between two *RXTE* observations taken on MJDs 54751.2 and 54752.1, then decayed monotonically again until it reached a minimum level on MJD 54786.2. As the onset of this second event is not resolved, we report an upper limit of 1 day for the rise time. This second flux enhancement decayed monotonically for $\sim$34 days; the pulsed count rate in this period can be parameterized by an exponential fall-off with $1/e$ decay time of $\sim$ 25 days, although a linear

[4] `http://www.atnf.csiro.au/research/pulsar/tempo/`

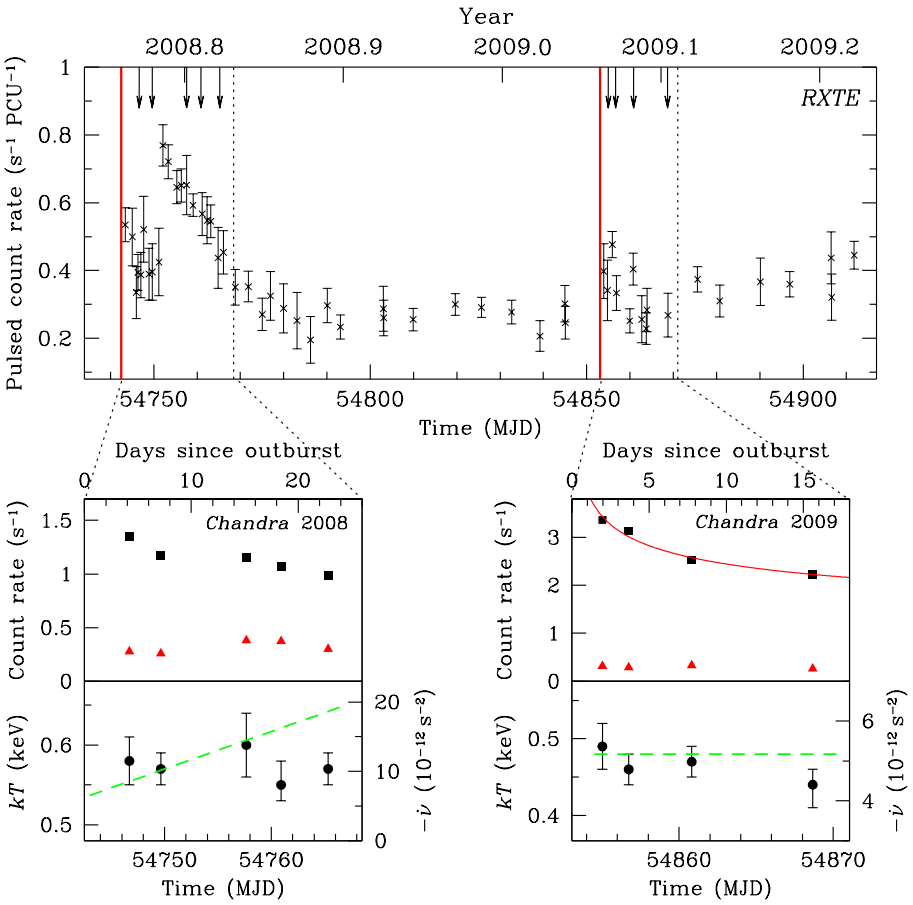

FIG. 1.— Top: rms pulsed flux of 1E 1547.0−5408 in the 2-10 keV range obtained with *RXTE*. The red vertical solid lines mark the outbursts in 2008 and 2009, and the arrows indicate the *Chandra* observation epochs. Bottom: total and rms pulsed *Chandra* count rates in the 1-7 keV band, shown by black squares and red triangles in the upper panels, respectively. The statistical uncertainties are negligible. The solid line in 2009 illustrates a power-law fit to the flux decay. Note that the first *Chandra* observation in 2009 was made with the HETG, which precludes a direct comparison of the count rates. Therefore, the data point plotted here is estimated from the spectral analysis results. The lower panels show the best-fit blackbody temperature from the PL+BB model, as listed in Table 2. The green dashed lines indicate the spin-down rate obtained from the phase-coherent *RXTE* timing solutions. Uncertainties in $\dot{\nu}$ measurements are negligible (at 1% level).

decay is also consistent with the data. Interestingly, the 2009 event, which is more energetic, is far less dramatic as seen by *RXTE*, with a relatively small increase in the pulsed flux observed.

2.2. Chandra *Observations and Results*

The 2008 outburst of 1E 1547.0−5408 triggered a series of *Chandra* observations through our Target of Opportunity (ToO) program. Five total pointings were made on days 4, 7, 15, 18 and 23 after the outburst, with exposures ranging from 12 to 23 ks. Data were taken with the ACIS-S detector in continuous clocking (CC) mode, which has a time resolution of 2.85 ms. For the 2009 event, another *Chandra* ToO program followed the outburst, with four ACIS-S CC mode observations taken on days 2, 4, 8 and 16. The first exposure in 2009 was taken with the High Energy Transmission Grating (HETG). We include only the zeroth-order events in this latter data set in our analysis. A summary of observation parameters is provided in Table 1.

We performed all the *Chandra* data reduction using CIAO 4.2 with CALDB 4.2.0. We first removed the burst intervals in the data. Source counts were extracted from a 3″ diameter aperture and background counts were from the whole chip excluding the central 40″ region (i.e., a total width of 7.′7). We note that although there is a nearby source XMMU J155053.7−541925 southwest to the pulsar (Gelfand & Gaensler 2007), the projected separation is always larger than 30″ in the CC-mode data. Therefore, it does not contaminate the source counts. The source count rates in the 1-7 keV energy range are reported in Table 1 and plotted in Figure 1, in which the backgrounds have been accounted for, although they are less than 0.5%. The count rates are well below the telemetry limit of *Chandra*, and pileup is negligible due to the short frame time of the CC-mode exposures. While the source flux changes between epochs, we found no short-term variability within any individual exposure. Employing a test algorithm suggested by Gregory & Loredo (1992), we found $< 10\%$ probability of source variability within individual observations, which is not statistically significant. The flux decay in 2009 can be modeled by a power law of index $\alpha = -0.21 \pm 0.01$, which is plotted in Figure 1. However, such a simple relation is not observed in the 2008 flux evolution. In particular, the count rates are very similar between the second and third exposures, which is likely related to the enhanced pulsed flux detected by *RXTE*.

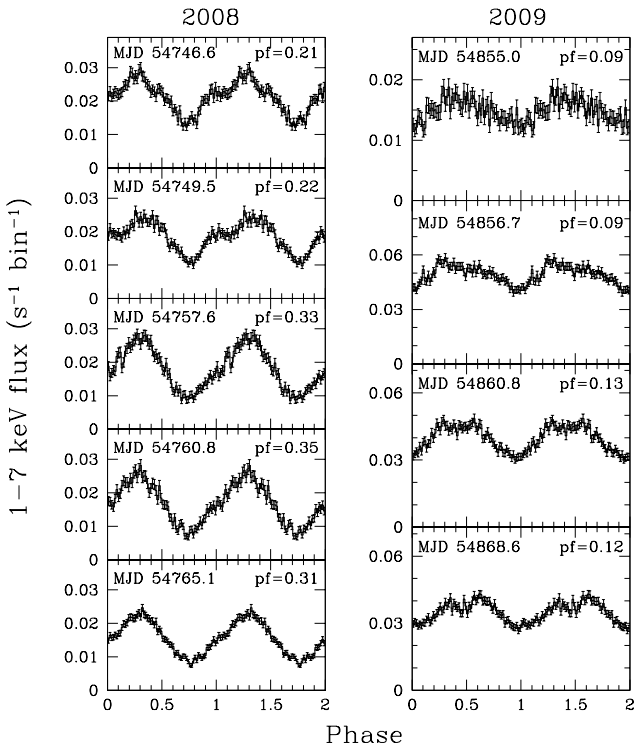

FIG. 2.— Pulse profiles of 1E 1547.0−5408 in 1-7 keV obtained from the *Chandra* observations, using 64 phase bins. The rms PFs from Table 1 are indicated.

2.2.1. *Chandra Timing*

We applied a barycenter correction to the *Chandra* data and then folded the photon arrival times according to the *RXTE* ephemeris. The resulting lightcurves are shown in Figure 2. The pulse profiles in 2008 suggest some hints of a multi-peak morphology in the first two observations, then evolve into a single peak. By contrast, the 2009 profiles exhibit a broad peak at first, with a second peak emerging by the third observation. We found no obvious energy dependence of the pulse shape across the *Chandra* band (0.5-10 keV). A direct comparison between the profiles in 2008 and 2009 indicates a much higher pulse modulation in the former. We estimated the rms pulsed fractions (PFs) in 1-7 keV, and the results are listed in Table 1. We observe a clear trend of increasing pulse modulation as the source recovers after the outbursts.

To look for energy dependence of the modulation, we estimated the PFs in the soft (1-3 keV) and hard (3-7 keV) energy bands separately. In the 2008 data, the latter shows a systematically higher PF, with a difference ranging from ΔPF = 0.04-0.09 (i.e., a 20%-30% change), which is statistically significant given the measurement uncertainty is only ∼0.01. However, such an energy dependence is not observed in 2009, with the PFs in the two bands being consistent with each other.

2.2.2. *Chandra Spectroscopy*

The *Chandra* spectra of 1E 1547.0−5408 were extracted using the tool `psextract` in CIAO, then binned such that every bin has an S/N of at least 10. We performed the spectral fits in the 0.5-7 keV range with XSPEC v12.6.0. All nine datasets were fitted jointly with a single absorption column density ($N_{\rm H}$). We also tried

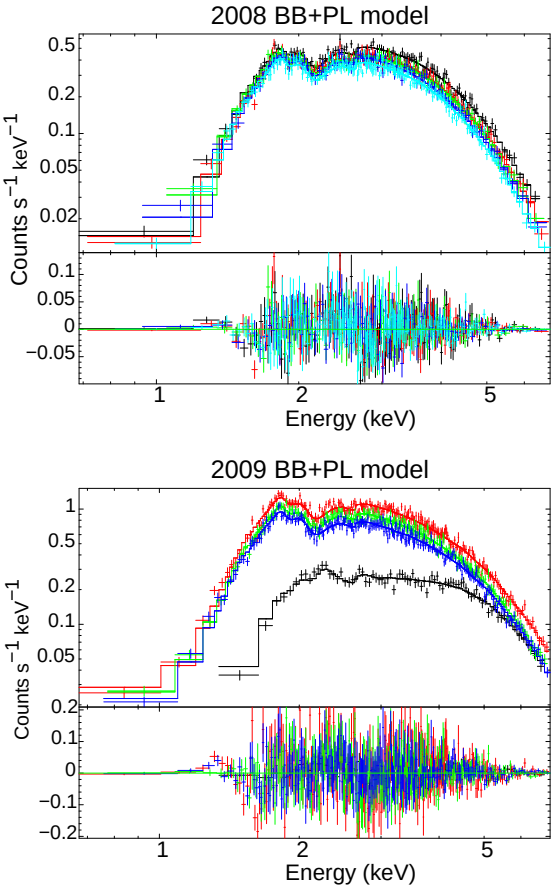

FIG. 3.— Best-fit blackbody plus power-law model fit to the 2008 and 2009 *Chandra* spectra (upper panels) with the corresponding residuals (lower panels). Different observations are shown by different colors. The corresponding best-fit spectral parameters are listed in Table 2.

fitting different $N_{\rm H}$ values for the 2008 and 2009 data, and confirmed that they are consistent. We started with simple models including an absorbed blackbody (BB) and an absorbed power-law (PL), but obtained very poor fits (reduced χ^2 values over 1.5). An absorbed blackbody plus power-law (BB+PL) model gives much better fits and the results are listed in Table 2 and plotted in Figure 3. As shown in the figure, the fit residuals suggest a hint of a spectral feature ∼ 1.3 keV, which is more obvious in 2009 than in 2008. However, the significance is only ∼1σ and deeper exposures are needed to confirm this.

In addition to the BB+PL model, we also considered more physical models that account for the Compton upscattering of the thermal photons in the magnetosphere. We tried fitting the Resonant Cyclotron Scattering (RCS; Lyutikov & Gavriil 2006; Rea et al. 2008) and the Surface Thermal Emission and Magnetospheric Scattering (STEMS; Özel 2003; Güver et al. 2006) models to the data. In the latter, the gravitational redshift is fixed at $z = 0.306$ during the fit, corresponding to the canonical neutron star mass of 1.4 $M_\odot$ and radius of 10 km. While these models fit the 2008 data reasonably well, the 2009 spectra clearly require an additional hard component. Therefore, we added a PL to the spectral model in 2009, with Γ fixed at 1.33 according to the *Suzaku*

TABLE 2
Phase-averaged Spectral Parameters of 1E 1547.0−5408 for Different Models

Obs.	$N_{\rm H}$ ($10^{22}\,{\rm cm}^{-2}$)	B ($10^{14}\,{\rm G}$)	kT (keV)	R (km)	Γ	$f^{\rm abs\ a}$ (10^{-11} erg s^{-1} cm^{-2})	$F_{\rm pl}/F_{\rm th}$ [b]	χ^2_ν/ν
Blackbody + power-law model								
2008								
1	4.1 ± 0.1[c]	···	0.58 ± 0.03	2.0 ± 0.3	$2.3^{+0.3}_{-0.4}$	1.92 ± 0.03	$1.4^{+1.0}_{-0.6}$	1.08/1342[c]
2	4.1 ± 0.1[c]	···	0.57 ± 0.02	$2.1^{+0.3}_{-0.2}$	$2.3^{+0.3}_{-0.4}$	1.64 ± 0.02	$1.1^{+0.8}_{-0.5}$	1.08/1342[c]
3	4.1 ± 0.1[c]	···	0.60 ± 0.04	$1.7^{+0.4}_{-0.3}$	2.8 ± 0.3	1.57 ± 0.03	$2.6^{+1.6}_{-1.1}$	1.08/1342[c]
4	4.1 ± 0.1[c]	···	$0.55^{+0.03}_{-0.02}$	$2.2^{+0.4}_{-0.3}$	$2.4^{+0.3}_{-0.5}$	1.55 ± 0.03	$1.2^{+1.1}_{-0.6}$	1.08/1342[c]
5	4.1 ± 0.1[c]	···	0.57 ± 0.02	1.8 ± 0.2	$2.8^{+0.2}_{-0.3}$	1.34 ± 0.02	$2.1^{+1.2}_{-0.8}$	1.08/1342[c]
2009								
6	4.1 ± 0.1[c]	···	0.49 ± 0.03	$4.4^{+0.8}_{-0.7}$	$2.0^{+0.3}_{-0.4}$	5.11 ± 0.09	$1.6^{+1.8}_{-0.8}$	1.08/1342[c]
7	4.1 ± 0.1[c]	···	0.46 ± 0.02	$4.7^{+0.7}_{-0.5}$	2.1 ± 0.2	4.61 ± 0.05	$1.8^{+1.0}_{-0.6}$	1.08/1342[c]
8	4.1 ± 0.1[c]	···	0.47 ± 0.02	$4.0^{+0.6}_{-0.5}$	2.3 ± 0.2	3.67 ± 0.04	$2.2^{+1.3}_{-0.8}$	1.08/1342[c]
9	4.1 ± 0.1[c]	···	$0.44^{+0.02}_{-0.03}$	$4.1^{+0.8}_{-0.6}$	2.4 ± 0.2	3.22 ± 0.04	$2.7^{+1.8}_{-1.0}$	1.08/1342[c]
RCS + hard power-law model								
2008								
1	4.0 ± 0.1[c]	···	$0.47^{+0.05}_{-0.04}$	···	···	1.91 ± 0.03	···	1.09/1338[c]
2	4.0 ± 0.1[c]	···	0.47 ± 0.04	···	···	1.63 ± 0.02	···	1.09/1338[c]
3	4.0 ± 0.1[c]	···	$0.38^{+0.07}_{-0.05}$	···	···	1.56 ± 0.03	···	1.09/1338[c]
4	4.0 ± 0.1[c]	···	$0.43^{+0.07}_{-0.03}$	···	···	1.53 ± 0.03	···	1.09/1338[c]
5	4.0 ± 0.1[c]	···	0.41 ± 0.04	···	···	1.33 ± 0.02	···	1.09/1338[c]
2009								
6	4.0 ± 0.1[c]	···	$0.32^{+0.05}_{-0.13}$	···	1.33[d]	5.11 ± 0.09	0.37 ± 0.08	1.09/1338[c]
7	4.0 ± 0.1[c]	···	$0.17^{+0.16}_{-0.04}$	···	1.33[d]	4.62 ± 0.05	$0.37^{+0.14}_{-0.12}$	1.09/1338[c]
8	4.0 ± 0.1[c]	···	$0.32^{+0.04}_{-0.16}$	···	1.33[d]	3.67 ± 0.03	$0.30^{+0.05}_{-0.09}$	1.09/1338[c]
9	4.0 ± 0.1[c]	···	$0.13^{+0.18}_{-0.01}$	···	1.33[d]	3.23 ± 0.04	$0.27^{+0.11}_{-0.08}$	1.09/1338[c]
STEMS + hard power-law model								
2008								
1	4.5 ± 0.1[c]	$2.61^{+0.10}_{-0.08}$	$0.313^{+0.011}_{-0.008}$	10[d]	···	1.90 ± 0.03	···	1.08/1329[c]
2	4.5 ± 0.1[c]	$2.69^{+0.10}_{-0.07}$	$0.314^{+0.011}_{-0.005}$	10[d]	···	1.62 ± 0.02	···	1.08/1330[c]
3	4.5 ± 0.1[c]	2.57 ± 0.06	$0.28^{+0.02}_{-0.06}$	10[d]	···	1.56 ± 0.03	···	1.08/1331[c]
4	4.5 ± 0.1[c]	$3.4^{+0.2}_{-0.3}$	$0.35^{+0.05}_{-0.02}$	10[d]	···	1.53 ± 0.03	···	1.08/1332[c]
5	4.5 ± 0.1[c]	$2.62^{+0.06}_{-0.04}$	$0.30^{+0.005}_{-0.07}$	10[d]	···	1.33 ± 0.02	···	1.08/1333[c]
2009								
6	4.5 ± 0.1[c]	$5.4^{+0.9}_{-1.4}$	$0.46^{+0.09}_{-0.13}$	10[†]	1.33[†]	5.08 ± 0.09	$0.21^{+0.09}_{-0.11}$	1.08/1334[c]
7	4.5 ± 0.1[c]	$3.01^{+0.12}_{-0.09}$	0.306 ± 0.003	10[†]	1.33[†]	4.60 ± 0.05	0.16 ± 0.02	1.08/1335[c]
8	4.5 ± 0.1[c]	$3.6^{+0.2}_{-0.1}$	$0.312^{+0.012}_{-0.002}$	10[†]	1.33[†]	3.66 ± 0.04	$0.12^{+0.03}_{-0.02}$	1.08/1336[c]
9	4.5 ± 0.1[c]	$3.0^{+0.6}_{-0.1}$	$0.30^{+0.02}_{-0.011}$	10[†]	1.33[†]	3.23 ± 0.04	$0.15^{+0.02}_{-0.01}$	1.08/1337[c]

Note. — All uncertainties quoted are 90% confidence intervals (i.e., 1.6σ).

[a] Absorbed flux in 0.5-7 keV range.

[b] Unabsorbed flux ratio between the power-law and the primary (i.e., blackbody, STEMS, or RCS) components in 0.5-7 keV range.

[c] All nine data sets were fitted jointly with a single column density.

[d] Held fixed in the fit.

results (Enoto et al. 2010).[5] Compared to the BB+PL fit above, these models provide a similar goodness-of-fit in terms of the reduced χ^2 values. Table 2 lists the key parameters of the best-fit models. The scattering optical depth τ is around 1-2 in 2008 and $\gtrsim 3$ in 2009, and the thermal velocity β of the electrons is ∼0.4-0.5 in 2008 and ~ 0.2 in 2009 (see Lyutikov & Gavriil 2006, for a detailed definition of these parameters).

3. DISCUSSION

In this paper, we have reported on *Chandra* observations of 1E 1547.0−5408 immediately following its 2008 and 2009 outbursts, along with *RXTE* timing and pulsed flux behavior following the 2008 outburst and throughout the 2009 event. Next we discuss these observations in the context of the magnetar model.

3.1. *Spectral and Spin Evolution*

In the twisted magnetosphere model of magnetars (Thompson et al. 2002), the observed X-ray luminosity of a magnetar is determined both by its surface temperature and by magnetospheric currents, the latter due to the twisted dipolar field structure. The surface temperature in turn is determined by the energy output from within the star due to magnetic field decay, as well as on the nature of the atmosphere and the stellar magnetic field strength. This surface thermal emission is resonantly scattered by the current particles, thus resulting in an overall spectrum similar to a

[5] The *INTEGRAL* results also suggest that the hard-band PL spectral index remained stable over the period of the *Chandra* observations (den Hartog et al. 2009).

Comptonized blackbody (e.g. Lyutikov & Gavriil 2006; Rea et al. 2008; Zane et al. 2009). In this model, the greater the twist angle, the greater the scattering, the harder the spectrum, and the greater the X-ray luminosity L_X. In addition, the surface heating by return currents is believed to contribute substantially to L_X, at least at the same level as the thermal component induced from the interior field decay (Thompson et al. 2002). Magnetar outbursts in this picture occur with sudden increases in twist angle, consistent with the generic hardening of magnetar spectra during outbursts (e.g. Kaspi et al. 2003; Woods et al. 2004; Israel et al. 2007).

Other observational evidence provided in support of the twisted magnetosphere model as proposed by Thompson et al. (2002) is a correlation between magnetar spectral hardness and spin-down-inferred magnetic field strength B, when comparing different sources (Marsden & White 2001; Kaspi & Boydstun 2010). In this case, B is an observational proxy for the magnetospheric twist angle. On the other hand, some magnetars have shown dramatic spin-down rate variations, with order-of-magnitude changes in $\dot{\nu}$ seen on a variety of timescales (e.g. Gavriil & Kaspi 2004; Woods et al. 2004). The origin of these variations is unknown. Nevertheless, in the context of the twisted magnetosphere model, a varying twist angle might naively be expected to be accompanied by a changing $\dot{\nu}$ (due to changing effective B), and corresponding spectral and flux changes. However, some decoupling between $\dot{\nu}$ and the radiative behavior might be expected, particularly as the spin-down is affected most by a narrow field-line bundle near the light cylinder, whereas the radiation originates from the surface. Field-line twists likely propagate outward (Thompson et al. 2002), which suggests the radiative changes should occur prior to $\dot{\nu}$ changes (Beloborodov & Thompson 2007).

In contrast to the picture in which a magnetar outburst is accompanied by an enhanced magnetospheric twist, Özel & Güver (2007) suggest that in outburst, the magnetosphere may be stable, with radiative evolution being due to changes in the surface thermal emission. Using a spectral model consisting of a resonant Comptonized atmosphere-modified blackbody (the STEMS model), fits to data for XTE J1810−197 (Güver et al. 2007) result in the spectrally inferred B being stable, with all radiative changes being due to changes in the surface thermal emission.

For 1E 1547.0−5408, the source spectrum only showed significant variability over a short period of time (∼1 day) following the 2008 and 2009 outbursts (Israel et al. 2010; Scholz et al., in preparation), but remained stable over the *Chandra* observations, during which the flux changed substantially (see Table 2). The latter seems opposite to the hardness/flux correlation predicted by the twisted magnetosphere model. On the other hand, we note that the flux decay over the *Chandra* epochs has a comparable timescale to that of the pulse profile variations (Figure 2), which generally agrees with the predictions of the magnetar model. More intriguing are the timing results. As described in Section 2.1.1, we found a factor of 2.2 increase in the spin-down rate $|\dot{\nu}|$ between the first and last *Chandra* observations in 2008, a substantial change even by magnetar standards. For purely dipole spin-down, this naively implies a ∼50% increase in the effective surface dipole field strength, from an initial spin-inferred value of 2.8×10^{14} G at the epoch of the first *Chandra* observation, to a value of 4.1×10^{14} G at the epoch of the last. This is contrary to SGR 1806−20, in which the spectral response lagged behind the torque variation, suggesting some hysteresis in the system (Woods et al. 2007). In our case, the lack of associated spectral changes is unexpected in the twisted magnetosphere model, unless the spin-down is decoupled from the site of the radiative events, as suggested by Gavriil & Kaspi (2004) for 1E 1048.1−5937 (see also Beloborodov 2009). Although B fields inferred from long-term spin-down have been used to compare with those inferred spectrally (e.g. Güver et al. 2007), our results call into question the reliability of such a comparison when using short-term spin-down rate.

Indeed, for the 2008 *Chandra* observations of 1E 1547.0−5408, spectral fits using the STEMS model yield a very similar B field value for all the observations (see Table 2) in spite of the strongly varying $\dot{\nu}$. One way to reconcile this is to interpret the B field measured spectroscopically as higher-order multipoles in localized X-ray-emitting regions rather than the global dipole field responsible for spin-down. However, we note that the B field obtained from the STEMS model is *lower* than the spin-down-inferred value at the epoch of the last 2008 *Chandra* observation, which is difficult to be explained by the above picture. As an alternative, the extra spin-down torque could be attributed to particle winds (Harding et al. 1999). Comparing the spin-down rates of 1E 1547.0−5408 in 2007 (Camilo et al. 2008), 2008 and 2009 (Section 2.1.1), it is obvious that the spin-down torque changed drastically between these epochs. Torque variations have been observed in magnetars and ordinary radio pulsars (e.g. Kaspi et al. 2003; Gavriil & Kaspi 2004; Kramer et al. 2006; Lyne et al. 2010; Livingstone et al. 2011). These could be related to changes in plasma conditions in the magnetosphere, which may not necessarily have any observable effects in the radiative properties (see **?**). Based on Equation (9) in Harding et al. (1999), a factor of 2.2 increase in $|\dot{\nu}|$, and hence in $\dot{E}$, requires a steady wind luminosity (L_p) 1.5 times larger than the dipole spin-down luminosity, implying $L_p \approx 1.5 \times 10^{35}$ ergs s^{-1}. For a typical X-ray efficiency of below 1%, the particle-induced flux would be less than 10^{-12} ergs cm^{-2} s^{-1}, much smaller when compared to the source's flux (see Table 2), thus, unlikely to be detected.

In any case, the absence of spectral variations in the presence of flux changes remains puzzling whether or not the magnetospheric twist angle varied in the outburst. Moreover, a reasonable model will need to explain why $\dot{\nu}$ changed drastically following the 2008 event, but stayed constant in 2009. This may reinforce the requirement of decoupling between the spin-down and the source of the radiative changes, hence presumably between the spin-down-inferred magnetic field and that inferred spectrally.

3.2. *Flux Evolution During the 2008 and 2009 Events*

The 2008 and 2009 events exhibited very different flux evolutions. Immediately after the 2009 outburst, the per-

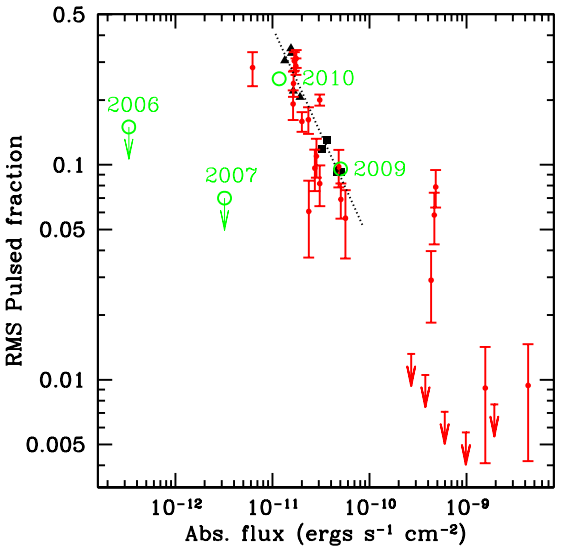

FIG. 4.— rms PF vs. absorbed flux of 1E 1547.0−5408 in the 1-7 keV band. The filled triangles and squares show the 2008 and 2009 *Chandra* observations, respectively. The green open circle and red dots represent results from *XMM-Newton* and *Swift*, respectively (Halpern et al. 2008; S. A. Olausen et al., in preparation; P. Scholz et al., in preparation), with the *XMM-Newton* epochs labeled. Note that the 2007 and 2008 *XMM-Newton* data points are only upper limits, since the values reported in the literature are area PF estimates, which are larger than the rms PFs by a constant which depends on the pulse shape. The dashed line shows a power-law fit to the *Chandra* data.

sistent flux increased by a factor of ~ 500 (Scholz et al. in preparation), while the pulsed flux evidently showed only very little variation (less than a factor of two). We found a monotonic flux decay during the 2009 recovery, with a power-law of index -0.21 ± 0.01, which is comparable to -0.306 ± 0.005 for CXOU J164710.2−455216 (Woods et al. 2011), but not as steep as -0.69 ± 0.03 for 1E 2259+586 (Zhu et al. 2008) or -0.92 ± 0.02 for XTE J1810−197 (Woods et al. 2005).

In contrast, the 2008 event is less energetic; the total flux increased only by a factor of ∼100 (Israel et al. 2010), but our *RXTE* results reveal a pulsed flux variation by a factor of ∼4, far greater than in the 2009 event. Also, the flux decay in 2008 showed a more complicated history. As is clear in Figure 1, we observed an additional flux enhancement around MJD 54752, ∼11 days after the initial trigger, [6] lasting for ∼30 days.

Eichler & Shaisultanov (2010) suggest that radiative outbursts in magnetars could generally be preceded by glitches, with the delay between the two events depending on the depth at which the glitch-induced energy release occurs. For the initial event in 2008, we are unable to tell whether a glitch preceded the radiative outburst, due to the lack of *RXTE* observations prior to the outburst. However, we can rule out any glitch between the initial 2008 event and the second flux enhancement 10 days later. It is possible that the initial event actually involved glitches occurring in two different places in the stellar interior, at substantially different depths, such that the delays from the glitch to the X-ray enhancement were different, but we note that this picture does not explain the sharp rise of the second flux enhancement.

[6] Although this second enhancement is not reported by Israel et al. (2010) in their study of the *Swift* observations covering the same period, we have re-analysed the same *Swift* dataset and confirmed the pulsed flux enhancement we observe with *RXTE* and *Chandra* (P. Scholz et al., in preparation).

3.3. *Pulsed Fraction Evolution*

Our results in Section 2 clearly indicate a strong anti-correlation between the PF and the phase-averaged X-ray flux, at least during the 2008 and 2009 outbursts. This is plotted in Figure 4, and suggests an approximate power-law relation between the two observables. The trend is also supported by the *XMM-Newton* and *Swift* measurements taken in the same period (S. A. Olausen et al., in preparation, P. Scholz et al., in preparation). Similar anti-correlations have been observed in 1E 1048.1−5937 and CXOU J164710.2−455216 (Tam et al. 2008; Israel et al. 2007), while positive correlations were found in XTE J1810−197 and 1E 2259+586 (Gotthelf et al. 2004; Zhu et al. 2008). This variety of behaviors is consistent with the picture in which, from source to source, the location and geometry of the region on the star affected in the outburst are different. Previous studies proposed that an anti-correlation could be the consequence of an increased emitting area due to an outburst, such that part of the hot spot becomes visible at any phase, thus reducing the pulse modulation (e.g. Halpern et al. 2008). We note that this scenario depends critically on the location of emission zone on the stellar surface as well as the viewing geometry (see Bogdanov et al. 2008); it may be possible to obtain either a monotonic increase or decrease of PF for the same area 'hot spot' depending on its location on the stellar surface.

We point out that the trend of decreasing PF for increasing phase-averaged X-ray flux observed in the *Chandra* data does not seem to hold for other observations of 1E 1547.0−5408 before 2008. Based on *XMM-Newton* exposures, Halpern et al. (2008) reported area PFs of 15% in quiescence in 2006 and 7% in the high state in 2007. As shown in Figure 4, these values deviate significantly from the 2008-2009 trend. The discrepancy seems too large to be reconciled by a difference in the instrument response, and is even larger if the differing PF estimate methods are accounted for. It is possible that the outburst in 2008 induced some permanent changes in the B-field configuration or emission geometry. The pulse profiles shown in Halpern et al. (2008) also appear to have a different shape from the ones shown in Figure 2, providing further support to this picture.

4. CONCLUSIONS

We have presented results from *Chandra* and *RXTE* observations of 1E 1547.0−5408 following its 2008 and 2009 outbursts. These allow a direct comparison between the two events. We found that over the 2008 *Chandra* observation epochs, the pulsar spin-down rate increased by a factor 2.2, in the absence of corresponding spectral changes, whereas such variation in $\dot{\nu}$ is not observed after the more energetic 2009 event. This provides evidence of decoupling between magnetar spin and radiative properties. The absence of spectral changes simultaneous with significant flux decay is surprising for models of magnetar outbursts. Our results also revealed a strong anti-correlation between the PF and phase-averaged flux of the source. While both 2008 and 2009 data follow

the same trend, pre-2008 measurements show significant deviation, suggesting that the 2008 outburst may have induced permanent changes in the emission geometry. Finally, we note that 1E 1547.0−5408 demonstrated significant spectral changes only within the first day after the 2008 and 2009 events, which highlights the importance of prompt observations in future studies for understanding post-outburst relaxation of magnetars.

We thank A. Archibald, S. Bogdanov, M. Livingstone and W. Zhu for useful discussions. C.-Y.N. is a CRAQ postdoctoral fellow. V.M.K. holds the Lorne Trottier Chair in Astrophysics and Cosmology and a Canada Research Chair in Observational Astrophysics. This work is supported by an NSERC Discovery Grant, by CIFAR, and by FQRNT via CRAQ.

Facilities: CXO (ACIS) RXTE (PCA)

REFERENCES

Beloborodov, A. M. 2009, ApJ, 703, 1044
Beloborodov, A. M., & Thompson, C. 2007, ApJ, 657, 967
Bogdanov, S., Grindlay, J. E., & Rybicki, G. B. 2008, ApJ, 689, 407
Camilo, F., Ransom, S. M., Halpern, J. P., & Reynolds, J. 2007, ApJ, 666, L93
Camilo, F., Reynolds, J., Johnston, S., Halpern, J. P., & Ransom, S. M. 2008, ApJ, 679, 681
den Hartog, P. R., Kuiper, L., & Hermsen, W. 2009, ATel, 1922
Dib, R., Kaspi, V. M., & Gavriil, F. P. 2008, in AIP Conf. Proc. 983, 40 Years of Pulsars: Millisecond Pulsars, Magnetars and More, ed. C. Bassa, Z. Wang, A. Cumming, & V. M. Kaspi, 239
Dib, R., Kaspi, V. M., & Gavriil, F. P. 2009, ApJ, 702, 614
Eichler, D., & Shaisultanov, R. 2010, ApJ, 715, L142
Enoto, T., et al. 2010, PASJ, 62, 475
Gavriil, F. P., & Kaspi, V. M. 2004, ApJ, 609, L67
Gavriil, F. P., Kaspi, V. M., & Woods, P. M. 2006, ApJ, 641, 418
Gelfand, J. D., & Gaensler, B. M. 2007, ApJ, 667, 1111
Gotthelf, E. V., Halpern, J. P., Buxton, M., & Bailyn, C. 2004, ApJ, 605, 368
Gregory, P. C., & Loredo, T. J. 1992, ApJ, 398, 146
Gronwall, C., Holland, S. T., Markwardt, C. B., Palmer, D. M., Stamatikos, M., & Vetere, L. 2009, GRB Coord. Netw., 8833, 1
Güver, T., Özel, F., Göğüş, E., & Kouveliotou, C. 2007, ApJ, 667, L73
Güver, T., Özel, F., & Lyutikov, M. 2006, arXiv:astro-ph/0611405
Halpern, J. P., Gotthelf, E. V., Reynolds, J., Ransom, S. M., & Camilo, F. 2008, ApJ, 676, 1178
Harding, A. K., Contopoulos, I., & Kazanas, D. 1999, ApJ, 525, L125
Israel, G. L., Campana, S., Dall'Osso, S., Muno, M. P., Cummings, J., Perna, R., & Stella, L. 2007, ApJ, 664, 448
Israel, G. L., et al. 2010, MNRAS, 408, 1387
Kaneko, Y., et al. 2010, ApJ, 710, 1335
Kaspi, V. M. 2007, Ap&SS, 308, 1
Kaspi, V. M., & Boydstun, K. 2010, ApJ, 710, L115
Kaspi, V. M., Gavriil, F. P., Woods, P. M., Jensen, J. B., Roberts, M. S. E., & Chakrabarty, D. 2003, ApJ, 588, L93
Kramer, M., Lyne, A. G., O'Brien, J. T., Jordan, C. A., & Lorimer, D. R. 2006, Science, 312, 549
Kuiper, L., den Hartog, P. R., & Hermsen, W. 2009, ATel, 1921
Lamb, R. C., & Markert, T. H. 1981, ApJ, 244, 94
Livingstone, L., Ng, C.-Y., Kaspi, V. M., Gariil, F. P., & Gotthelf, E. V. 2011, ApJ, submitted (arXiv:1007.2829)
Lyne, A., Hobbs, G., Kramer, M., Stairs, I., & Stappers, B. 2010, Science, 329, 408
Lyutikov, M., & Gavriil, F. P. 2006, MNRAS, 368, 690
Marsden, D., & White, N. E. 2001, ApJ, 551, L155
Mereghetti, S. 2008, A&AR, 15, 225
Mereghetti, S., et al. 2009, ApJ, 696, L74
Özel, F. 2003, ApJ, 583, 402
Özel, F., & Güver, T. 2007, ApJ, 659, L141
Rea, N., Zane, S., Turolla, R., Lyutikov, M., & Götz, D. 2008, ApJ, 686, 1245
Savchenko, V., Neronov, A., Beckmann, V., Produit, N., & Walter, R. 2010, A&A, 510, A77
Tam, C. R., Gavriil, F. P., Dib, R., Kaspi, V. M., Woods, P. M., & Bassa, C. 2008, ApJ, 677, 503
Terada, Y., et al. 2009, GRB Coord. Netw., 8845, 1
Thompson, C., Lyutikov, M., & Kulkarni, S. R. 2002, ApJ, 574, 332
Tiengo, A., et al. 2010, ApJ, 710, 227
Woods, P. M., Kaspi, V. M., Gavriil, F. P., & Airhart, C. 2011, ApJ, submitted (arXiv:1006.2950)
Woods, P. M., Kouveliotou, C., Finger, M. H., Göğüş, E., Wilson, C. A., Patel, S. K., Hurley, K., & Swank, J. H. 2007, ApJ, 654, 470
Woods, P. M., et al. 2004, ApJ, 605, 378
—. 2005, ApJ, 629, 985
Zane, S., Rea, N., Turolla, R., & Nobili, L. 2009, MNRAS, 398, 1403
Zhu, W., Kaspi, V. M., Dib, R., Woods, P. M., Gavriil, F. P., & Archibald, A. M. 2008, ApJ, 686, 520